HHS Public Access

Author manuscript

J Immunol. Author manuscript; available in PMC 2017 January 01.

Published in final edited form as:

J Immunol. 2016 January 1; 196(1): 80–90. doi:10.4049/jimmunol.1501537.

Glucose oxidation is critical for CD4+ T cell activation in a mouse model of systemic lupus erythematosus[1]

Yiming Yin[#], **Seung-Chul Choi**[#], **Zhiwei Xu**, **Leilani Zeumer**, **Nathalie Kanda**, **Byron P. Croker**, and **Laurence Morel**[*]

Department of Pathology, Immunology, and Laboratory Medicine, University of Florida, Gainesville, FL 32610, USA

Abstract

We have previously shown that $CD4^+$ T cells from B6.Sle1.Sle2.Sle3 (TC) lupus mice and patients present a high cellular metabolism, and a treatment combining 2-deoxyglucose (2DG), which inhibits glucose metabolism, and metformin, which inhibits oxygen consumption, normalized lupus T cell functions *in vitro* and reverted disease in mice. We obtained similar results with B6.*lpr* mice, another model of lupus, and showed that a continuous treatment is required to maintain the beneficial effect of metabolic inhibitors. Further, we investigated the relative roles of glucose oxidation and pyruvate reduction into lactate in this process.. Treatments of TC mice with either 2DG or metformin were sufficient to prevent autoimmune activation, while their combination was necessary to reverse the process. Treatment of TC mice with dichloroacetate (DCA), an inhibitor of lactate production, failed to effectively prevent or reverse autoimmune pathology. *In vitro*, $CD4^+$ T cell activation upregulated the expression of genes that favor oxidative phosphorylation. Blocking glucose oxidation inhibited both IFNγ and IL-17 production, which could not be achieved by blocking pyruvate reduction. Overall, our data shows that targeting glucose oxidation is required to prevent or reverse lupus development in mice, which cannot be achieved by simply targeting the pyruvate-lactate conversion.

Keywords

Lupus; T cells; metabolism; autoimmunity; glucose; metformin

Introduction

$CD4^+$ T cells undergo activation, proliferation and differentiation upon antigen exposure. Depending on cytokine signals, $CD4^+$ T cells can differentiate into effector T cell (Teff) lineages, such as Th1, Th2 and Th17 cells, or regulatory T cells (Treg). Teff cells contribute to the immune response by producing pro-inflammatory cytokines, whereas Treg cells

[1]This study was supported by NIH grants R01 AI045050 and ALR-TIL 0000075018 to LM.

[*]Corresponding author: Laurence Morel, Department of Pathology, Univ. of Florida, 1395 Center Drive, Gainesville, FL 32610-0275. Tel: (352) 273-5638. Fax: (352) 392-3053. morel@ufl.edu.

[#]These authors contributed equally to the study

Disclosures

The authors declare that they have no conflict of interest.

suppress immunity and inflammation. Overactive Teff cells and pro-inflammatory cytokine production have been implicated in the pathogenesis of systemic lupus erythematosus (SLE) (1). Studies in SLE patients and murine models of lupus have shown increased frequencies of Th1 and Th17 cells, as well as enhanced level of IFNγ and IL-17 (2–4). Mice deficient in either IFNγ (5–7) or IL-17 (8, 9) are protected from autoantibodies production and development of glomerulonephritis (GN). Therefore, targeting Teff cells such as Th1 and Th17 cells represents a promising strategy for treating SLE (10).

To support activation, proliferation and differentiation, $CD4^+$ T cells need to meet large needs in energy and biosynthesis. Glucose is a major source for energy and biosynthesis in activated $CD4^+$ T cells (11). After transport into cells, glucose undergoes a ten-step reaction to generate pyruvate. Pyruvate utilization is an important regulatory point of glucose metabolism, as it can either be reduced into lactate by lactate dehydrogenase (*Ldha*) in the cytosol, or transported into the mitochondria via the mitochondria pyruvate carrier (MPC) complex (12, 13). Within the mitochondria, pyruvate is converted into acetyl-coA by the pyruvate dehydrogenase complex (PDC), a process that is tightly regulated by the pyruvate dehydrogenase kinase (*Pdk1*), which can phosphorylate PDC and inhibit its activity. Upon activation, $CD4^+$ T cells quickly increased glucose uptake and metabolism, leading to increased lactate production (14, 15). However, whether $CD4^+$ T cell activation and effector function requires pyruvate oxidation is unclear, and current data are inconsistent. It has been proposed that pyruvate oxidation decreases $CD4^+$ T cell activation (15). This result was however obtained with exogenous pyruvate. On the other hand, glucose oxidation is required for Th17 polarization to support *de novo* fatty acid synthesis (16). Deficiency in Estrogen Related Receptor Alpha (*Esrra*), a transcription factor orchestrating cellular metabolism, decreased pyruvate oxidation and impaired $CD4^+$ T cell function (17). Furthermore, T cell activation leads to increased mitochondrial oxygen consumption (15, 18), which could be at least partly due to enhanced pyruvate oxidation. Given these inconsistent data, the role of pyruvate metabolism in $CD4^+$ T cell functions needs to be examined in further details.

We have reported an enhanced lactate production and mitochondrial oxygen consumption in the $CD4^+$ T cells from B6.NZM.*Sle1*.*Sle2*.*Sle3* (TC) lupus-prone mice as well as SLE patients (19). We showed that blocking glucose metabolism with 2-Deoxy-D-glucose (2DG) in combination with metformin (Met) reverted disease in these mice, but neither 2DG or Met alone were effective in mice with established disease (19). The mechanisms of action of Met are complex (20), but, within the dose-range that we used, Met inhibits the mitochondrial complex 1 and oxidative phosphorylation (OXPHOS) (21). This is consistent with our findings that Met decreases oxygen consumption in T cells (19). Met also normalized the excessive production of IFNγ by $CD4^+$ T cells from TC mice and SLE patients (19). This suggested a critical involvement of mitochondrial hyperactivity in lupus T cells. In support of this hypothesis, mitochondrial membrane hyperpolarization, an indication of high mitochondrial metabolism, was reported in T cells from SLE patients (22). In addition, increased pyruvate oxidation by $CD4^+$ T cells has been demonstrated in mouse models of SLE (23).

Here, we report that CD4+ T cells from B6.lpr mice, another model of spontaneous lupus, have also a high metabolism, and that Met+2DG was effective in reversing immune pathology as it did in TC mice. We also provide evidence for a critical role of mitochondrial metabolism and pyruvate oxidation in the regulation of TC $CD4^+$ T cells. The selective inhibition of pyruvate conversion into lactate by dichloroacetate (DCA) was less effective than the inhibition of glucose metabolism by 2DG in either preventing or reverting disease in TC mice. Moreover, we showed that the *in vitro* activation of $CD4^+$ T cells enhanced pyruvate oxidation in addition to lactate production. By using small molecule inhibitors, we showed that pyruvate oxidation is important for IFNγ production, whereas both pyruvate oxidation and its conversion into lactate are important for IL-17A production. Overall, these results provided new insights into how glucose metabolism regulates T cell function and autoimmunity, and revealed the importance of glucose oxidation in lupus development.

Methods

Mice and *in vivo* treatments

TC mice have been described previously (18). B6 and B6.MRL-Fas^{lpr}/J (B6.*lpr*) mice were originally purchased from the Jackson Laboratory. Only female mice were used in this study at the age indicated for each experiment. Treatment was performed with metabolic inhibitors (all from Sigma) dissolved in drinking water: Met (3 mg/mL), 2DG (5 mg/mL), dichloroacetate (DCA, 2mg/ml) or a combination of two of these drugs for the duration indicated for each study. For each treatment study, contemporaneous age-matched control mice received plain drinking water. Preventive treatments were performed in 2 month old mice, and reversal treatments were performed in mice at least 7 month of age and all anti-dsDNA IgG positive for TC mice, and 4 month of age for B6.*lpr* mice. Peripheral blood was collected to analyze autoantibody production; body weight and blood sugar levels were monitored weekly and biweekly respectively. At the end of the treatment, spleens were collected for flow cytometry and metabolic analysis of $CD4^+$ T cells, and kidneys were evaluated for renal pathology. All experiments were conducted according to protocols approved by the University of Florida IACUC.

Metabolic measurements

Splenocyte suspensions were enriched for $CD4^+$ T cells by negative selection with magnetic beads (Miltenyi) yielding $CD4^+$ cell population with a purity >90%. Extracellular acidification rate (ECAR) and oxygen consumption rate (OCR) were measured using with a XF96 Extracellular Flux Analyzer under mitochondrial stress test conditions (Seahorse). Assay buffer was made of non-buffered RPMI medium supplemented with 2.5 uM dextrose, 2 mM glutamine and 1 uM sodium pyruvate (all from Sigma). Baseline ECAR and OCR values were averaged between at least 4 technical replicates per sample for the first 3 successive time intervals. In some assays, T cells were stimulated for 24 hr with plate-bound anti-CD3e (2 ug/ml) and soluble anti-CD28 (1 ug/ml) in RPMI before analysis.

Flow Cytometry

Single-cell suspensions were prepared from spleens using standard procedures. After red blood cell lysis, cells were blocked with anti-CD16/32 Ab (2.4G2), and stained in FACS

staining buffer (2.5% FBS, 0.05% sodium azide in PBS). Fluorochrome-conjugated Abs used were to B220 (RA3-6B2), BCL6 (K112-91), CD4 (RAM4-5), CD25 (PC61.5), CD44 (IM7), CD62L (MEL-14), CD69 (H1.2F3), CD95 (Jo2), CD122 (TM-b1), CD152 (UC10-4B9), CD154 (MR1), FOXP3 (FJK-16s), ICOS (15F9), IFN-γ (XMG1.2), IL-17A (TC11-18H10.1), Ly-77 (GL7), PD-1 (RMP1-30), purchased from BD Biosciences, eBioscience, and BioLegend. Follicular T cells were stained as previously described (55) in a three-step process using purified CXCR5 (2G8) followed by biotinylated anti-rat IgG (Jackson ImmunoResearch) and PerCP5.5-labeled streptavidin in FACS staining buffer on ice. Dead cells were excluded with fixable viability dye (eFluor780, eBioscience). Data were collected on LSRFortessa (BD Biosciences) and analyzed with FlowJo (Tree Star) or FCS Express (DeNovo) software. IFN-γ and IL-17A production were analyzed in cells treated with the leukocyte activation cocktail (BD Biosciences) for 5 h and the Fixation/ Permeabilization kit (eBiosciences).

Cell Culture

Freshly isolated splenic $CD4^+$ T cells (5×10^5 per well) were polarized for 3 d with plate-bound anti-CD3e (2 ug/ml) and soluble anti-CD28 (1 ug/ml) in RPMI. Th1 polarization was performed by adding IL-12 (10 ng/ml) and anti-IL-4 (10 ug/ml), and Th17 polarization was performed by adding TGFβ (3 ng/ml), IL-6 (50 ng/ml), 6-Formylindolo (3,2-b) carbazole (FICZ, 300 nM; Enzo Life Sciences), anti-IL-4 and anti-IFNγ (10 ug/ml each). Metabolic inhibitors (all from Sigma), Met (1 mM), 2DG (1 mM), DCA (10 mM), UK5099 (10 uM) or troglitazone (10 uM), were added to the cell cultures at the beginning of polarization. Gene expression for metabolic enzymes was measured by quantitative RT-PCR using Sybr Green incorporation as previously indicated (19).

Antibody measurement

Serum anti-dsDNA and anti-chromatin IgG were measured by ELISA and anti-nuclear autoAb (ANA) were measured by immunofluorescence on Hep-2 cells as previously described (24). To normalize for inter-individual variations in short-term treatments, anti-dsDNA IgG levels were compared for each mouse as percent change from the initial pre-treatment value. ANA images were acquired with the same settings on an immunofluorescence microscope and mean fluorescence intensity (MFI) was computed with ImageJ (imagej.nih.gov/ij) after background subtraction.

Renal pathology

GN was scored semi-quantitatively in a blind fashion by a renal pathologist (BPC) as previously described (25). Briefly, the type of lesion was scored by order of increasing severity: none, mesangial matrix (Mm), mesangial cellular (Mc) and proliferative global (Pg) GN and the extent of the lesions was score on a scale 1 to 4. The glomerular deposition of C3 and IgG immune complexes was performed on frozen kidney sections as previously described (25). Glomerular size and the extent of C3 or IgG deposits were measured from sections averaging 3–6 glomeruli per sample, using Metamorph 7.5 (BioImaging Solutions).

Statistical Analysis

Statistical analyses were performed using the GraphPad Prism 6.0 software. Unless indicated, data was normally distributed, and graphs show means and standard deviations of the mean (SEM) for each group. Results were compared with 2-tailed *t* tests with a minimal level of significance set at $P < 0.05$. Bonferroni corrections were applied for multiple comparisons. Time-course results were compared by 2-way ANOVA. Each *in vitro* experiment was performed at least twice with reproducible results.

Results

Met+2DG treatment decreased autoimmune pathology in B6.*lpr* mice

To address whether the combination of Met + 2DG was effective in other models of lupus, we selected B6.*lpr* mice, a simplified model driven by FAS-deficiency and characterized by an expansion of $CD4^-$ $CD8^-$ double negative (DN) T cells. As TC T cells, $CD4^+$ T cells from B6.*lpr* mice showed an elevated aerobic glycolysis as shown by extracellular acidification (ECAR, Fig. 1A) as well as oxygen consumption (OCR, Fig. 1B). Similar results were obtained after *in vitro* activation of $CD4^+$ T cells from young mice with anti-CD3 and CD28 antibodies (Fig. 1C and D), with B6.*lpr* $CD4^+$ T cells maintaining a high spare respiratory capacity (SRC, Fig. 1E). The Met+2DG treatment for 7 weeks of anti-dsDNA IgG-positive mice decreased significantly decreased $CD4^+$ T cell ECAR (11.73 + 0.91 vs. 17.58 + 1.24 mpH/min, $p < 0.001$) and OCR (74.19 + 2.30 vs. 103.6 + 13.51 pMoles/min, $p < 0.05$). The treatment also limited lymphoid expansion (Fig. 1F) and prevented serum anti-dsDNA IgG (Fig. 1G) and ANA (Fig. 1H) to increase. Renal pathology is very mild in B6.*lpr mice*, however, the Met+2DG treatment limited the extent of IgG immune complexes deposited in the glomeruli (Fig. 1I) and limited glomerular expansion (Fig. 1J), a marker of lupus nephritis. The treatment did not affect the percentage of DN T cells (Fig. 1K), but it decreased the percentage of $CD4^+$ T cells (10.98 + 0.54 vs. 15.27 + 0.50 %, $p = 0.002$) as well as their activation (Fig. 1L). Met+2DG did not affect the large percentage of T_{EM} cells, but expanded the percentage of naïve $CD44^-$ $CD62L^+$ T_N cells (Fig. 1M) and decreased the percentage of T_{FH} cells (Fig. 1N). Accordingly, the percentages of GC B cells as well as plasma cells (PC) were decreased by the treatment (Fig. 1O). These results showed that an increased T cell metabolism is not restricted to the TC model of lupus, but also applies to the B6.*lpr* model, in which autoimmunity arises from a completely different pathway. In addition, the Met+2DG treatment was also effective in reducing lymphoid expansion, autoAb production and renal pathology in B6.*lpr* mice.

Cessation of Met+2DG treatment resulted in flares

We have shown that a 5h *in vitro* treatment with Met was sufficient to reduce IFNγ production (19), suggesting that T cells respond rapidly to metabolism alterations. It is unknown, however, whether the *in vivo* Met+2DG treatment re-set the immune system or, to the contrary, whether a continuous treatment is required to maintain therapeutic benefits. To address this question, we performed a reversal Met+2DG treatment for 8 weeks, then the treated mice were split into three cohorts: same Met+2DG treatment or plain water for 2 or 6 additional weeks, and compared to age-matched mice that were never treated. As previously reported (19), the Met+2DG treatment decreased splenomegaly (Fig. 2A), anti-dsDNA IgG

(Fig. 2B), renal pathology (Fig. 2C), $CD4^+$ T cell activation (Fig. 2D and E), follicular helper T cell (T_{FH}, Fig. 1F) and germinal center (GC) B cell expansion (Fig. 2G). However, the therapeutic effects of disappeared after the treatment was stopped for as little as 2 weeks (Fig. 2), showing that $CD4^+$ T cells required continuous exposure to Met+2DG to downregulate their activation and effector differentiation. We tested this hypothesis *in vitro* by comparing the continuous effect of Met for 6 d to only for the first 3 d on Th1 polarization (Fig. 1H). The removal of Met in the last 3 d resulted in a percentage of $CD4^+$ T cells expressing IFNγ and a level of expression that were equivalent to that of cells that were never treated with Met. These values were significantly higher than that of cells maintained on Met for 6 d in both strains. Overall, these results indicate that continuous inhibition of T cell metabolism is required to maintain the anti-inflammatory effect.

Monotherapy with either Met or 2DG prevented disease development

We have shown that monotherapy with either Met or 2DG did not reverse disease in TC mice (19). To assess whether any of these drugs was able to prevent autoimmune activation and pathology to develop, we treated TC mice and B6 controls starting at 8 weeks of age. Met treatment for 22 weeks resulted in a greater body weight gain in TC mice (Fig. 3A), but had no effect in B6 (data not shown), suggesting that the weight gain in Met-treated mice may be associated with a decreased morbidity. Accordingly, Met reduced splenomegaly (calculated as spleen to body weight ratio to account for the difference in body weight, Fig. 3B). The production of anti-dsDNA (Fig. 3C) and anti-chromatin (Fig. 2D) IgG remained below pre-treatment levels until the last two weeks of treatment. Terminal serum ANAs were also significantly decreased by the treatment (Fig. 3E). $CD4^+$ T cell activation (Fig. 3F and G) and T_{FH} cell expansion (Fig. 3H) were reduced by the Met treatment, and there was a trend for a reduction of GC B cells (Fig. 3I). The severity of renal pathology was also significantly reduced with a shift to mesangial from proliferative GN (Fig. 3J). Similarly, we treated 8 week old TC mice with 2DG for 16 weeks, and observed a modest but significant weight gain (Fig. 4A) as well as a reduced lymphoid expansion in the spleen (Fig. 4B) of treated mice. Serum anti-dsDNA IgG remained low in treated mice and significantly lower than in control mice (Fig. 4C and D). Similarly, terminal serum ANAs were decreased by the treatment (Fig. 4E). Finally, $CD4^+$ T cell activation (Fig. 4F and G), T_{FH} cell and GC B cell expansion (Fig. 4H and I), and the severity of renal pathology (Fig. 4J) were all reduced by 2DG. These results showed that either Met or a global reduction of glucose metabolism were sufficient to prevent autoimmune activation and pathology in TC mice.

Inhibition of pyruvate reduction does not prevent or reverse lupus

To determine whether the reduction of pyruvate to lactate was the critical branch of glucose metabolism in TC T cells, we used dichloroacetate (DCA), an inhibitor of PDK1, which inhibits pyruvate dehydrogenase (PDH) and pyruvate oxidation (26). The resulting effect of DCA is to favor the oxidation of pyruvate to the expense of its conversion to lactate (27, 28). DCA globally decreased $CD4^+$ T cell metabolism with a greater effect on glycolysis than OXPHOS (Fig. 5 A and B), leading to a lower ECAR/OCR ratio (Fig 5C). Eight week old TC mice were treated with DCA or 2DG for 16 weeks and compared to age-matched controls. As expected, 2DG reduced both ECAR and OCR in the $CD4^+$ T cells of treated mice, but no difference was observed for DCA-treated mice (Fig. 5D–E). This preventive

DCA treatment had no significant effect on lymphoid expansion (Fig. 5F), anti-dsDNA IgG production (Fig. 5G), $CD4^+$ T cell activation and differentiation (Fig. 5H–J), as well as GC B cell induction (Fig. 5K). Finally, DCA had no significant effect on the expression of key T cell activation markers as compared to 2DG (Fig. 5L-O). Therefore, inhibiting pyruvate reduction did not recapitulate the effect of inhibiting of the entire glucose metabolism in developing lupus.

We further evaluated the effect of DCA treatment on disease reversal either as monotherapy. Eight month old TC mice were treated with DCA or Met for 2 months and compared to age-matched controls. In older mice, the DCA treatment significantly reduced aerobic glycolysis while increasing OXPHOS, leading to a shift toward mitochondrial metabolism in $CD4^+$ T cells (Fig. 6A). In these mice, DCA resulted in body weight loss (Fig. 6B) and lymphoid expansion (Fig. 6C). DCA treatment had either no effect or increased autoAb levels (Fig. 6D–F), and had no effect on $CD4^+$ T cell activation and differentiation (Fig. 6G–J) or GC B cell expansion (Fig. 6K). DCA also did not change the expression of surface markers on $CD4^+$ T cells (Fig. 6L–O) and renal pathology (Fig. 6P). Finally, we compared the combination of Met+DCA to the Met+2DG treatment to assess whether the effective branch of glucose metabolism blocked by 2DG was aerobic glycolysis (Sup. Fig. 1). The Met+DCA treatment, however, did not change $CD4^+$ T cell metabolism (Sup. Fig. 1A–B), most likely due to the opposite effects of the two drugs on glucose metabolism. There was only a significant decrease in the expansion of T_{EM} cells (Sup. Fig. 1H), but all the other biomarkers, including renal pathology, were unchanged. Overall, these results showed that the inhibition of pyruvate reduction to lactate by DCA, even in combination with metformin, is not effective in preventing or reverting autoimmune pathology in TC mice, suggesting that lactate production is not the critical glycolytic pathway in the $CD4^+$ T cells of TC mice.

$CD4^+$ T cell activation increases pyruvate oxidation

The results from *in vivo* treatments suggested that OXPHOS is an important pathway relative to pyruvate reduction to lactate for $CD4^+$ T cell activation in the TC model of lupus. Consistent with this hypothesis, thiazolidinediones (TZD) reduced T cell activation, ANA production and renal pathology in SLE (29, 30), which has been attributed to their peroxisome proliferator-activated receptor gamma (PPARγ) agonist activity (22). However, TZDs have been recently shown to be acute MPC inhibitors, effectively shutting down pyruvate oxidation (31, 32). Interestingly, pioglitazone (a TZD) normalized IFNγ but not IL-17 production in T cells from lupus patients (29), suggesting a different requirement of pyruvate oxidation in these two T cell subsets. To further test how pyruvate utilization regulates $CD4^+$ T cells function, we compared the expression of key metabolic genes between *in vitro* activated and untouched naïve $CD4^+$ B6 T cells (Fig. 7A). Anti-CD3/CD28 activation significantly upregulated *Hk2* expression confirming that T cell activation increases glucose metabolism. Activated $CD4^+$ T cells also showed a higher expression of lactate dehydrogenase A (*Ldha*) and lactate transporter MCT4 (*Slc16a3*), confirming an increased conversion of pyruvate into lactate. Importantly, we also observed a significant down-regulation of *Pdk1* levels, indicating an increased pyruvate oxidation. Anti-CD3/CD28 activation also strongly upregulated *Gls2* and *Odc*, confirming the upregulation of glutamine metabolism in activated $CD4^+$ T cells (15). In contrast, *Cpt1a* levels were down-

regulated, indicating a decreased fatty acid oxidation. Thus, these results showed that *in vitro* $CD4^+$ T cell activation increased glutamine and glucose metabolism, with both pyruvate oxidation and reduction into lactate. To investigate whether $CD4^+$ T cell activation depends on pyruvate oxidation under different cytokine environment, we measured the expression of the same metabolic genes after Th1, Th17 and Treg polarization in both B6 and TC $CD4^+$ T cells (Fig. 7B). Metabolic enzyme expression was globally similar between the two strains in all three polarized subsets, except for *Slc16a3*, *Pdk1* and *Gls2*, which were significantly lower in polarized TC than B6 T cells. These results support a skewing toward pyruvate oxidation in TC T cells. Importantly, all activated and polarized subsets presented a significantly lower *Pdk1* expression, as well as a higher *Gls2* and *Odc* expression compared to naïve cells (Fig. 7B). This suggested a higher involvement of both glucose and glutamine oxidation in all subsets. Therefore, increased substrate oxidation is a general feature of T cell activation *in vitro*, regardless of polarizing condition.

Finally, we assessed the requirement of pyruvate oxidation for IFNγ and IL-17A production using *in vitro* polarization in the presence of pharmacological inhibitors. In addition to DCA, we used two MPC inhibitors, UK5099 and troglitazone (a TZD), that are expected to have an effect opposite to DCA, i.e. blocking pyruvate oxidation vs. blocking lactate production. Consistent with a previous report (26), DCA inhibited IL-17A production (Fig. 8A and B) and increased Foxp3 expression (data not shown) in Th17-polarized B6 T cells. The same result was obtained with TC T cells, although IL-17A production remained higher than in B6 T cells. In addition, TZD, UK5099 and Met significantly inhibited IL-17A production in these conditions (Fig. 8A and B). This data indicates that disruption of either lactate production or OXPHOS, including pyruvate oxidation, impairs IL-17A production. In contrast, DCA significantly enhanced the percentage of $CD4^+$ T cells producing IFNγ (Fig. 8A and C) as well as the amount of IFNγ produced (Fig. 8D and E) in Th1-polarized TC and B6 T cells. As we previously reported (19), Met reduced IFNγ production (Fig. 8C). The same result was obtained with UK5099 and TZD, These data suggest that both IFNγ and IL-17 production depends on pyruvate oxidation, and IL-17 production also relies on lactate production. Therefore, Th1 and Th17 cells have different requirement on glucose metabolism. Inhibition of glucose reduction by DCA selectively targets Th17, whereas inhibition of MPC targets both Th1 and Th17 cells. These results also explain why DCA was not as effective as 2DG in the *in vivo* treatments.

Discussion

In this study, we first showed that $CD4^+$ T cell metabolism was elevated in B6.*lpr* mice, another model of lupus with a different etiology that the TC model, which includes a strong contribution of Th17 cells (33). Furthermore, the same Met+2DG treatment was effective in suppressing autoimmune manifestations in B6.*lpr* mice, although neither the effector memory nor DN T cells were affected. The treatment was very effective in reducing the number and percentage of Tfh cells in both strains. Follicular helper T cells have been identified as a strong disease biomarker in human SLE (34, 35), and their functional metabolism depends on both glucose metabolism and OXPHOS (36). The effectiveness of Met+2DG in the two lupus models may be linked to the targeting of this T cell subset. Nonetheless, our results showed that T cell metabolic defects in SLE are not model-

dependent and suggest that treatments with metabolic inhibitors may be beneficial in patients with a range of etiologies. We also showed that the therapeutic benefit of Met+2DG rapidly disappears when treatment is stopped. We have previously shown that a 5h *in vitro* treatment with Met is sufficient to inhibit IFNγ production by $CD4^+$ T cells (19). This and our new *in vivo* results demonstrated that the activation of lupus T cells is tightly controlled by their energy state, and removal of metabolic blocks quickly leads to reactivation and differentiation into effector subsets. Our results also showed that treatment with metabolic inhibitors do not reset the immune system, which has consequences for future translational studies.

Activation of $CD4^+$ T cells increases both lactate production and OXPHOS (15, 18). A number of studies have shown that the differentiation into inflammatory effector $CD4^+$ T cells, especially Th1 and Th17 cell subsets, relies on aerobic glycolysis (11, 37). Multiple studies have also shown that $CD4^+$ T cell activation requires mitochondrial metabolism, specifically OXPHOS and ROS production (18, 38). The relative contribution of these metabolic pathways to lupus pathogenesis has both mechanistic and translational implications. Indeed, most of the studies regarding the metabolic requirements of effector $CD4^+$ T cells have been conducted with either *in vitro* studies or with short-term acute autoimmune inductions such as the EAE model. Contrary to what we have reported in disease reversal studies (19), monotherapy with either 2DG or Met effectively prevented or significantly delayed disease in TC mice. This indicates that $CD4^+$ T cells that have been chronically activated by autoantigens require the inhibition of both glucose metabolism and mitochondrial oxidation to be normalized, but this activation can be prevented by targeting either pathway. The fact that autoimmune activation and pathology were prevented by Met suggests that the conversion of pyruvate to lactate, which is not targeted by Met (19), is not critical in this process. $CD4^+$ T cell activation only requires OXPHOS, but once activated, $CD4^+$ T cells can use either OXPHOS or aerobic glycolysis (39). In light of these findings, our results indicate that the activation of autoimmune TC $CD4^+$ T cells can be prevented by blocking glucose OXPHOS with either 2DG or Met. Then both 2DG and Met are required to normalize chronically activated $CD4^+$ T cells to inhibit both aerobic glycolysis and OXPHOS. The lack of efficacy of Met+DCA treatment comparatively to Met+2DG suggests that the first ten steps of glycolysis (i.e. conversion of glucose to pyruvate) are important for the activation of TC T cells. This is most likely due to the production of NADPH through the pentose phosphate pathway and the synthesis of amino acids and nucleotides from glyceraldehyde 3-phosphate, two key pathways for macromolecule synthesis that are mobilized in activated T cells (40). In addition, other sources of OXPHOS that are blocked by Met but not by 2DG may be involved. Anaplerotic glutamine metabolism is critical for $CD4^+$ T cell activation, both *in vitro* (41) and *in vivo* (42). It is therefore likely that glutaminolysis also contributes to the activation of lupus T cells, which should be tested in future reversal studies combining glucose and glutamine inhibitors.

Our *in vitro* studies have specifically compared pyruvate oxidation and reduction in $CD4^+$ T cell activation and polarization into Th1 and Th17 subsets. After activation, $CD4^+$ T cells up-regulated *Hk2*, *ldh2*, and *Slc16a3*, but down-regulated *Pdk1*, indicating that both lactate production and pyruvate oxidation were enhanced after $CD4^+$ T cell activation. Th1 and

Th17 polarization was associated with the downregulation of *Pdk1* and up-regulation of *Gls2* and *Odc*, indicating the prevalence of mitochondrial metabolism fueled by pyruvate and glutamine for IFNγ and IL-17A production. These results were confirmed with metabolic inhibitors probing pyruvate utilization, showing that both IFNγ and IL-17A were targeted by MPC inhibitors. IL-17A is however different from IFNγ in that it also requires pyruvate reduction. Overall, our results combining gene expression and metabolic inhibitors suggest that pyruvate oxidation is critical for T cell activation and inflammatory cytokine production. A previous study has found that neither ATP production nor a functioning electron transport chain was required for IFNγ production (39), but the inhibitors were added to cells already polarized, when we have shown that metformin was less effective (and therefore mitochondrial oxidation was less required) than when polarization is initiated (19). A recent proteomic study of Th1-polarized human $CD4^+$ T cells showed a drastic upregulation of pyruvate oxidation and TCA cycle utilization (43), confirming our results showing a strong involvement of mitochondrial oxidation in IFNγ production. Our *in vitro* results suggest that both glucose and glutamine are involved, but their respective contribution to the spontaneous chronic activation of lupus T cells remains to be determined.

IFNγ is the dominant cytokine produced by $CD4^+$ T cells in the TC mouse model of lupus (19). The enhancement of IFNγ production by DCA is likely a major reason why treatment with this metabolic inhibitor was not effective as 2DG in this model. Other models of lupus are dominated by other types of effector T cells. Th17 cells play a dominant role in B6.*lpr* mice (33), and therefore DCA may be more effective, although we have shown that the combination of Met and 2DG is effective at suppressing autoAb production and preventing the development of early renal pathology. The BXSB.Yaa model is dominated by Tfh cells (44, 45) and type I IFN (46). It will be therefore very informative to assess the efficacy of metabolic inhibitors in these other models of SLE.

In summary, we provide evidence that glucose oxidation plays a significant role in the activation of $CD4^+$ T cells in the TC mouse model of lupus and the inhibition of this metabolic pathway is critical to normalize their function and the associated autoimmune pathology. This is similar to the graft vs. host disease (GVHD) model, in which T cells chronically activated by alloantigens increased both aerobic glycolysis and OXPHOS, but an ATP synthase inhibitor was sufficient to block GVHD (47). We propose that mitochondrial oxidation of glucose, and potentially glutamine, are critical to sustain T cells chronically activated by autoantigens.

Supplementary Material

Refer to Web version on PubMed Central for supplementary material.

Acknowledgments

We thank Drs. Todd Brusko, Daniel Perry and Clayton Mathews from the University of Florida, Department of Pathology, Immunology, and Laboratory Medicine, and the members of the Morel laboratory for stimulating discussions

Abbreviations

2DG	2-Deoxy-D-glucose
ANA	anti-nuclear autoAb
B6	C57BL/6J mice
DCA	dichloroacetate
ECAR	extracellular acidification rate
GC	germinal center
GN	glomerulonephritis
MPC	mitochondrial pyruvate carrier
Met	metformin
OCR	oxygen consumption rate
OXPHOS	oxidative phosphorylation
ROS	reactive oxygen species
SLE	systemic lupus erythematosus
TC	B6.NZM.*Sle1*.*Sle2*.*Sle3* mice
Teff	effector T cells
T_{EM}	$CD44^+CD62L^-CD4^+$ effector memory T cells
T_{FH}	$CXCR5^+PD\text{-}1^+BCL6^+FOXP3^-CD4^+$ follicular helper T cells
Treg	regulatory T cells
TZD	thiazolidinedione

References

1. Moulton VR, Tsokos GC. T cell signaling abnormalities contribute to aberrant immune cell function and autoimmunity. J Clin Invest. 2015; 125:2220–2227. [PubMed: 25961450]
2. Ohl K, Tenbrock K. Regulatory T cells in systemic lupus erythematosus. Eur J Immunol. 2015; 45:344–355. [PubMed: 25378177]
3. Crispín JC, Tsokos GC. Interleukin-17-producing T cells in lupus. Curr Opin Rheumatol. 2010; 22:499–503. [PubMed: 20592603]
4. Pollard KM, Cauvi DM, Toomey CB, Morris KV, Kono DH. Interferon-gamma and systemic autoimmunity. Discov Med. 2013; 16:123–131. [PubMed: 23998448]
5. Richards HB, Satoh M, Jennette JC, Croker BP, Yoshida H, Reeves WH. Interferon-gamma is required for lupus nephritis in mice treated with the hydrocarbon oil pristane. Kidney Int. 2001; 60:2173–2180. [PubMed: 11737591]
6. Haas C, Ryffel B, Le Hir M. IFN-gamma receptor deletion prevents autoantibody production and glomerulonephritis in lupus-prone (NZB x NZW)F1 mice. J Immunol. 1998; 160:3713–3718. [PubMed: 9558072]
7. Peng S, Moslehi J, Craft J. Roles of interferon-gamma and interleukin-4 in murine lupus. J Clin Invest. 1997; 99:1936–1946. [PubMed: 9109438]
8. Zhang Z V, Kyttaris C, Tsokos GC. The role of IL-23/IL-17 axis in lupus nephritis. J Immunol. 2009; 183:3160–3169. [PubMed: 19657089]

9. Amarilyo G, Lourenço EV, Shi FD, La Cava A. IL-17 Promotes Murine Lupus. J Immunol. 2014; 93:540–543. [PubMed: 24920843]
10. Comte D, Karampetsou MP, Tsokos GC. T cells as a therapeutic target in SLE. Lupus. 2015; 24:351–363. [PubMed: 25801878]
11. MacIver NJ, Michalek RD, Rathmell JC. Metabolic regulation of T lymphocytes. Annu Rev Immunol. 2013; 31:259–283. [PubMed: 23298210]
12. Bricker DK, Taylor EB, Schell JC, Orsak T, Boutron A, Chen YC, Cox JE, Cardon CM, Van Vranken JG, Dephoure N, Redin C, Boudina S, Gygi SP, Brivet M, Thummel CS, Rutter J. A mitochondrial pyruvate carrier required for pyruvate uptake in yeast, Drosophila, and humans. Science. 2012; 337:96–100. [PubMed: 22628558]
13. Herzig S, Raemy E, Montessuit S, Veuthey JL, Zamboni N, Westermann B, Kunji ER, Martinou JC. Identification and functional expression of the mitochondrial pyruvate carrier. Science. 2012; 337:93–96. [PubMed: 22628554]
14. Frauwirth KA, Riley JL, Harris MH, Parry RV, Rathmell JC, Plas DR, Elstrom RL, June CH, Thompson CB. The CD28 signaling pathway regulates glucose metabolism. Immunity. 2002; 16:769–777. [PubMed: 12121659]
15. Wang R, Dillon CP, Shi LZ, Milasta S, Carter R, Finkelstein D, McCormick LL, Fitzgerald P, Chi H, Munger J, Green DR. The transcription factor Myc controls metabolic reprogramming upon T lymphocyte activation. Immunity. 2011; 35:871–882. [PubMed: 22195744]
16. Berod L, Friedrich C, Nandan A, Freitag J, Hagemann S, Harmrolfs K, Sandouk A, Hesse C, Castro CN, Bahre H, Tschirner SK, Gorinski N, Gohmert M, Mayer CT, Huehn J, Ponimaskin E, Abraham WR, Muller R, Lochner M, Sparwasser T. De novo fatty acid synthesis controls the fate between regulatory T and T helper 17 cells. Nat Med. 2014; 20:1327–1333. [PubMed: 25282359]
17. Michalek RD V, Gerriets A, Nichols AG, Inoue M, Kazmin D, Chang CY, Dwyer MA, Nelson ER, Pollizzi KN, Ilkayeva O, Giguere V, Zuercher WJ, Powell JD, Shinohara ML, McDonnell DP, Rathmell JC. Estrogen-related receptor-α is a metabolic regulator of effector T-cell activation and differentiation. Proc Natl Acad Sci U S A. 2011; 108:18348–18353. [PubMed: 22042850]
18. Sena LA, Li S, Jairaman A, Prakriya M, Ezponda T, Hildeman DA, Wang CR, Schumacker PT, Licht JD, Perlman H, Bryce PJ, Chandel NS. Mitochondria are required for antigen-specific T cell activation through reactive oxygen species signaling. Immunity. 2013; 38:225–236. [PubMed: 23415911]
19. Yin Y, Choi SC, Xu Z, Perry DJ, Seay H, Croker BP, Sobel ES, Brusko TM, Morel L. Normalization of CD4+ T cell metabolism reverses lupus. Sci Transl Med. 2015; 7:274ra218.
20. He L, Wondisford Fredric E. Metformin Action: Concentrations Matter. Cell Metabolism. 2015; 21:159–162. [PubMed: 25651170]
21. Mehta MM, Chandel NS. Targeting metabolism for lupus therapy. Sci Transl Med. 2015; 7:274fs275.
22. Perl A, Gergely P Jr, Nagy G, Koncz A, Banki K. Mitochondrial hyperpolarization: a checkpoint of T-cell life, death and autoimmunity. Trends Immunol. 2004; 25:360–367. [PubMed: 15207503]
23. Wahl DR, Petersen B, Warner R, Richardson BC, Glick GD, Opipari AW. Characterization of the metabolic phenotype of chronically activated lymphocytes. Lupus. 2010; 19:1492–1501. [PubMed: 20647250]
24. Morel L, Croker BP, Blenman KR, Mohan C, Huang G, Gilkeson G, Wakeland EK. Genetic reconstitution of systemic lupus erythematosus immunopathology with polycongenic murine strains. Proc Natl Acad Sci U S A. 2000; 97:6670–6675. [PubMed: 10841565]
25. Xu Z, Cuda CM, Croker BP, Morel L. The NZM2410-derived lupus susceptibility locus Sle2c1 increases TH17 polarization and induces nephritis in Fas-deficient mice. Arthritis Rheum. 2011; 63:764–774. [PubMed: 21360506]
26. Gerriets VA, Kishton RJ, Nichols AG, Macintyre AN, Inoue M, Ilkayeva O, Winter PS, Liu X, Priyadharshini B, Slawinska ME, Haeberli L, Huck C, Turka LA, Wood KC, Hale LP, Smith PA, Schneider MA, MacIver NJ, Locasale JW, Newgard CB, Shinohara ML, Rathmell JC. Metabolic programming and PDHK1 control CD4+ T cell subsets and inflammation. J Clin Invest. 2015; 125:194–207. [PubMed: 25437876]

27. Kaplon J, Zheng L, Meissl K, Chaneton B, Selivanov VA, Mackay G, van der Burg SH, Verdegaal EM, Cascante M, Shlomi T, Gottlieb E, Peeper DS. A key role for mitochondrial gatekeeper pyruvate dehydrogenase in oncogene-induced senescence. Nature. 2013; 498:109–112. [PubMed: 23685455]

28. Michelakis ED, Sutendra G, Dromparis P, Webster L, Haromy A, Niven E, Maguire C, Gammer TL, Mackey JR, Fulton D, Abdulkarim B, McMurtry MS, Petruk KC. Metabolic modulation of glioblastoma with dichloroacetate. Sci Transl Med. 2010; 2:31ra34.

29. Zhao W, Berthier CC, Lewis EE, McCune WJ, Kretzler M, Kaplan MJ. The peroxisome-proliferator activated receptor-γ agonist pioglitazone modulates aberrant T cell responses in systemic lupus erythematosus. Clin Immunol. 2013; 149:119–132. [PubMed: 23962407]

30. Aprahamian T, Bonegio RG, Richez C, Yasuda K, Chiang LK, Sato K, Walsh K, Rifkin IR. The Peroxisome Proliferator-Activated Receptor γ Agonist Rosiglitazone Ameliorates Murine Lupus by Induction of Adiponectin. J Immunol. 2009; 182:340–346. [PubMed: 19109165]

31. Divakaruni AS, Wiley SE, Rogers GW, Andreyev AY, Petrosyan S, Loviscach M, Wall EA, Yadava N, Heuck AP, Ferrick DA, Henry RR, McDonald WG, Colca JR, Simon MI, Ciaraldi TP, Murphy AN. Thiazolidinediones are acute, specific inhibitors of the mitochondrial pyruvate carrier. Proc Natl Acad Sci U S A. 2013; 110:5422–5427. [PubMed: 23513224]

32. Colca JR, McDonald WG, Cavey GS, Cole SL, Holewa DD, Brightwell-Conrad AS, Wolfe CL, Wheeler JS, Coulter KR, Kilkuskie PM, Gracheva E, Korshunova Y, Trusgnich M, Karr R, Wiley SE, Divakaruni AS, Murphy AN, Vigueira PA, Finck BN, Kletzien RF. Identification of a mitochondrial target of thiazolidinedione insulin sensitizers (mTOT)--relationship to newly identified mitochondrial pyruvate carrier proteins. PLoS One. 2013; 8:e61551. [PubMed: 23690925]

33. Kyttaris VC, Zhang Z, Kuchroo VK, Oukka M, Tsokos GC. Cutting edge: IL-23 receptor deficiency prevents the development of lupus nephritis in C57BL/6-lpr/lpr mice. J Immunol. 2010; 184:4605–4609. [PubMed: 20308633]

34. He J, Tsai LM, Leong YA, Hu X, Ma CS, Chevalier N, Sun X, Vandenberg K, Rockman S, Ding Y, Zhu L, Wei W, Wang C, Karnowski A, Belz GT, Ghali JR, Cook MC, Riminton DS, Veillette A, Schwartzberg PL, Mackay F, Brink R, Tangye SG, Vinuesa CG, Mackay CR, Li Z, Yu D. Circulating precursor CCR7(lo)PD-1(hi) CXCR5(+) CD4(+) T cells indicate Tfh cell activity and promote antibody responses upon antigen reexposure. Immunity. 2013; 39:770–781. [PubMed: 24138884]

35. Choi JY, Ho JH, Pasoto SG, Bunin V, Kim ST, Carrasco S, Borba EF, Goncalves CR, Costa PR, Kallas EG, Bonfa E, Craft J. Circulating follicular helper-like T cells in systemic lupus erythematosus: association with disease activity. Arthritis Rheumatol. 2015; 67:988–999. [PubMed: 25581113]

36. Ray, John P.; Staron, Matthew M.; Shyer, Justin A.; Ho, P-C.; Marshall, Heather D.; Gray, Simon M.; Laidlaw, Brian J.; Araki, K.; Ahmed, R.; Kaech, Susan M.; Craft, J. The interleukin-2-mTORc1 kinase axis defines the signaling, differentiation, and metabolism of T helper 1 and follicular B helper T cells. Immunity. Sep 21. pii: S1074-7613(15)00349-0. Epub ahead of print. 10.1016/j.immuni.2015.08.017

37. Pearce EL, Pearce EJ. Metabolic pathways in immune cell activation and quiescence. Immunity. 2013; 38:633–643. [PubMed: 23601682]

38. Weinberg SE, Sena LA, Chandel NS. Mitochondria in the regulation of innate and adaptive immunity. Immunity. 2015; 42:406–417. [PubMed: 25786173]

39. Chang CH, Curtis JD, Maggi LB Jr, Faubert B, Villarino AV, O'Sullivan D, Huang SC, van der Windt GJ, Blagih J, Qiu J, Weber JD, Pearce EJ, Jones RG, Pearce EL. Posttranscriptional control of T cell effector function by aerobic glycolysis. Cell. 2013; 153:1239–1251. [PubMed: 23746840]

40. Pearce EL, Poffenberger MC, Chang CH, Jones RG. Fueling immunity: insights into metabolism and lymphocyte function. Science. 2013; 342:1242454. [PubMed: 24115444]

41. Wang R, Dillon CP, Shi LZ, Milasta S, Carter R, Finkelstein D, McCormick LL, Fitzgerald P, Chi H, Munger J, Green DR. The transcription factor Myc controls metabolic reprogramming upon T lymphocyte activation. Immunity. 2011; 35:871–882. [PubMed: 22195744]

42. Glick GD, Rossignol R, Lyssiotis CA, Wahl D, Lesch C, Sanchez B, Liu X, Hao LY, Taylor C, Hurd A, Ferrara JLM, Tkachev V, Byersdorfer CA, Boros L, Opipari AW. Anaplerotic

metabolism of alloreactive T cells provides a metabolic approach to treat graft-versus-host disease. J Pharmacol Exp Therap. 2014; 351:298–307. [PubMed: 25125579]

43. Pagani M, Rockstroh M, Schuster M, Rossetti G, Moro M, Crosti M, Tomm JM. Reference proteome of highly purified human Th1 cells reveals strong effects on metabolism and protein ubiquitination upon differentiation. Proteomics. 2015 Sep.1 Epub ahead of print. 10.1002/pmic.201400139
44. Bubier JA, Sproule TJ, Foreman O, Spolski R, Shaffer DJ, Morse HC, Leonard WJ, Roopenian DC. A critical role for IL-21 receptor signaling in the pathogenesis of systemic lupus erythematosus in BXSB-Yaa mice. Proc Natl Acad Sci U S A. 2009; 106:1518–1523. [PubMed: 19164519]
45. Subramanian S, Tus K, Li QZ, Wang A, Tian XH, Zhou J, Liang C, Bartov G, McDaniel LD, Zhou XJ, Schultz RA, Wakeland EK. A Tlr7 translocation accelerates systemic autoimmunity in murine lupus. Proc Natl Acad Sci U S A. 2006; 103:9970–9975. [PubMed: 16777955]
46. Moisini I, Huang W, Bethunaickan R, Sahu R, Ricketts PG, Akerman M, Marion T, Lesser M, Davidson A. The Yaa locus and IFN-alpha fine-tune germinal center B cell selection in murine systemic lupus erythematosus. J Immunol. 2012; 189:4305–4312. [PubMed: 23024275]
47. Gatza E, Wahl DR, Opipari AW, Sundberg TB, Reddy P, Liu C, Glick GD, Ferrara JLM. Manipulating the Bioenergetics of Alloreactive T Cells Causes Their Selective Apoptosis and Arrests Graft-Versus-Host Disease. Science Translational Medicine. 2011; 3:67ra68–67ra68.

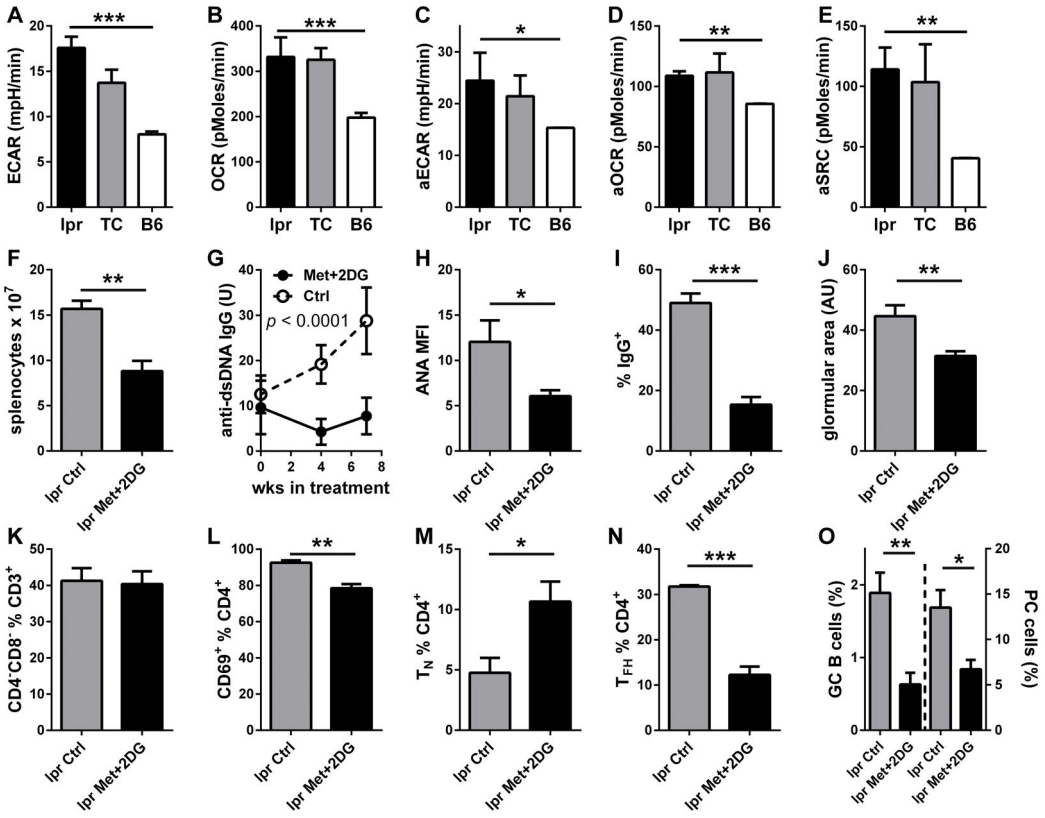

Figure 1. Met+2DG treatment decreased autoimmune pathology in B6.*lpr* mice

Basal ECAR (**A**) and OCR (**B**) in $CD4^+$ T cells from 6-month old mice (N = 4–10 per strain). Basal activated aECAR (**C**), aOCR (**D**) and aSRC (**E**) in $CD4^+$ T cells from 2-month old mice after 24 h activation with anti-CD3 and anti-CD28 antibodies (N = 3 per strain)**. F–O:** 4-month old B6.lpr mice were treated with Met+2DG for 7 weeks (N = 5), when analysis was performed comparatively to age-matched controls (N =4). **F**. Splenocyte numbers. **G**. Effect of treatment on serum anti-dsDNA IgG. **H**. ANA levels measured as MFI in terminal sera. **I**. Percentage of glomerular area with IgG deposits. **J**. Glomerular surface area measured in arbitrary units (AU). Percentage of $CD4^-$ $CD8^-$ DN T cells (**K**) $CD69^+$ (**L**), $CD44^-$ $CD62L^+$ T_N (**M**), $CXCR5^+$ $PD\text{-}1^+$ $BCL6^+$ $FOXP3^-$ T_{FH} (**N**) $CD4^+$ T cells and percentage of $CD95^+$ $GL7^+$ GC $B220^+$ B cells and PC (**O**). * $p < 0.05$, ** $p < 0.01$, *** $p < 0.001$.

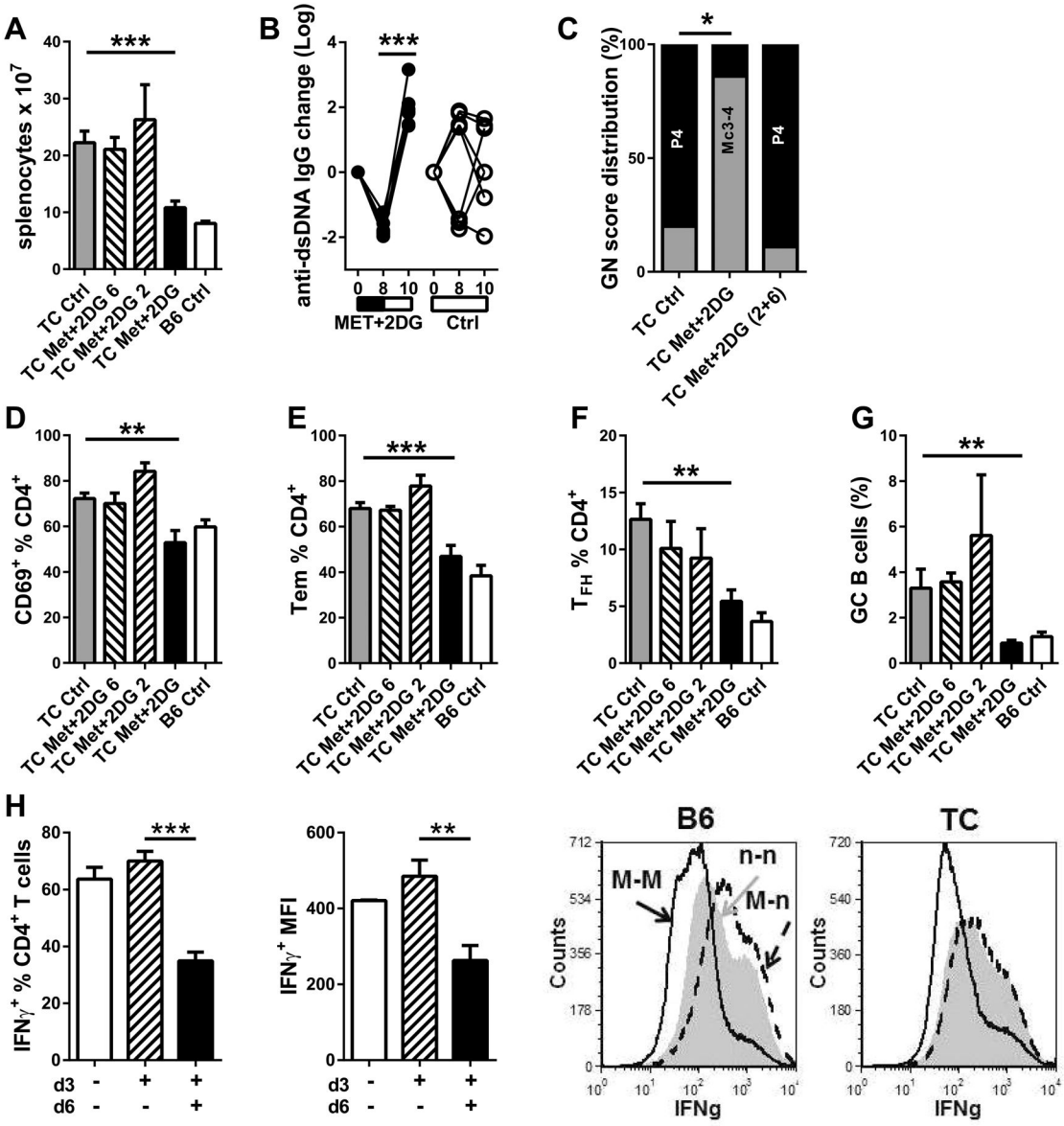

Figure 2. Cessation of Met+2DG treatment resulted in flares

8-month old TC mice were treated with Met+2DG for 8 weeks, then mice were maintained on treatment (Met+2DG), or switched to plain water for an additional 2 or 6 weeks (Met +2DG 2 and Met+2DG 6). Untreated TC and B6 mice (Ctrl) were analyzed at the same time. **A**. Splenocyte numbers. **B**. Changes in individual serum anti-dsDNA IgG levels in mice in which treatment ceased for 2 weeks as compared to untreated mice. **C**. GN score distribution: P4: proliferative GN score 4; Mc3-4: Mesangial cellular score 3 and 4 (grouped Met+2DG 2 and Met+2DG 6). Percentages of $CD69^+$ (**D**), $CD44^+$ $CD62L^-$ T_{EM} (**E**), and T_{FH} (**F**) $CD4^+$ T cells. **G**. Percentages $B220^+$ B cells with a GC phenotype. N = 4–8 per group. **H**. B6 and TC $CD4^+$ T cells were polarized *in vitro* with Met for 3 d, then washed and split into two fractions cultured in the same Th1 conditions with (black) or without (hatched) Met for an additional 3 d. Their percentage of $IFN\gamma^+$ $CD4^+$ T cells, as well as

level of Mean fluorescence intensity (MFI) of the IFNγ^+ production was compared to that of cells polarized for 6 d without Met (white). Representative FACS overlays are shown on the right for each strain. N = 3 per strain. ** $p < 0.01$, *** $p < 0.001$.

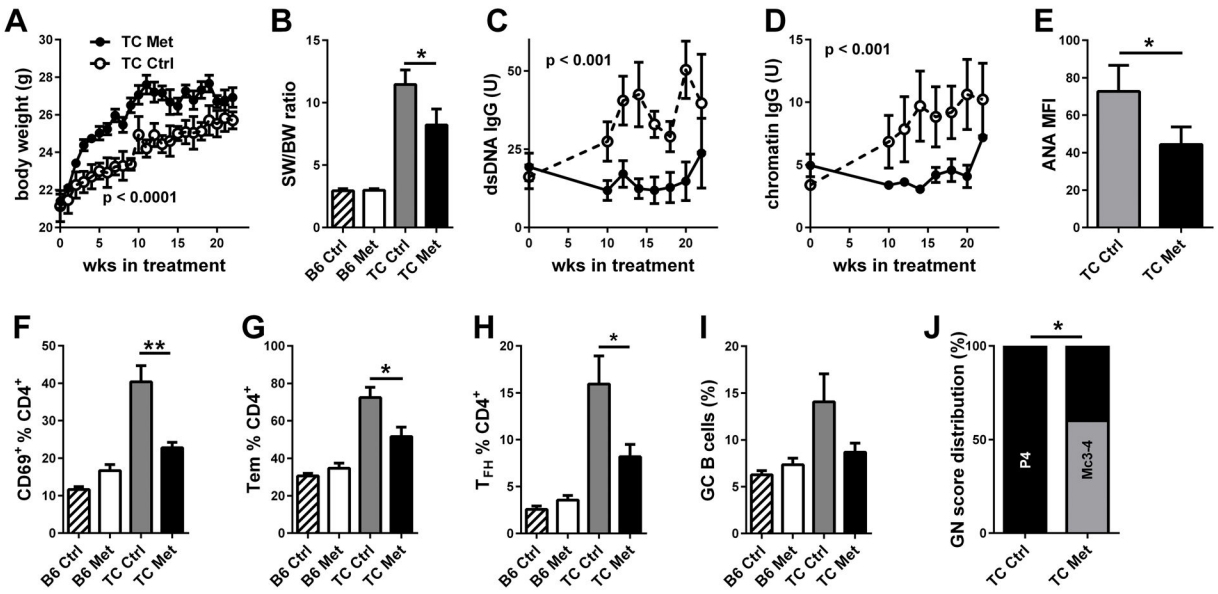

Figure 3. Met reduced the development of autoimmune pathogenesis

TC and B6 mice were treated with Met from 8 to 30 weeks of age, when analysis was performed. **A**. Effect of treatment on body weight in TC mice. **B**. Spleen weight to body weight ratio. Effect of treatment on serum anti-dsDNA (**C**) and chromatin (**D**) IgG in TC mice. **E**. ANA levels measured as MFI in terminal sera from TC mice. Percentage of $CD69^+$ (**F**), T_{EM} (**G**), and T_{FH} (**H**) $CD4^+$ T cells. **I**. Percentage $B220^+$ B cells with a GC phenotype. **J.** GN score distribution: P4: proliferative GN score 4; Mc3-4: Mesangial cellular score 3 and 4. N = 5 per group. * $p < 0.05$, ** $p < 0.01$.

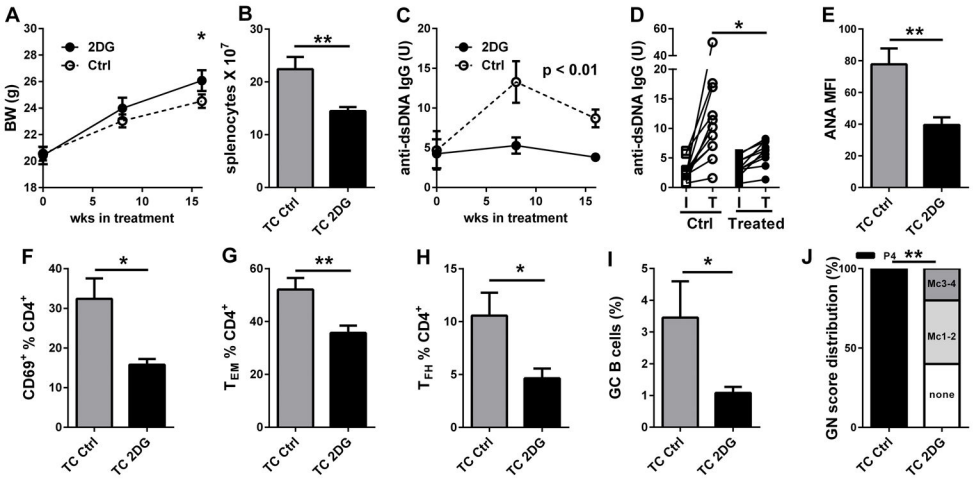

Figure 4. 2DG treatment reduced the development of autoimmune pathogenesis

TC mice were treated with 2DG from 8 to 24 weeks of age, when analysis was performed. **A**. Effect of treatment on body weight. **B**. Splenocytes numbers. Effect of treatment on serum anti-dsDNA IgG during the course of treatment (**C**) and for individual mice with initial (I) and terminal (T) values (**D**). **E**. ANA levels measured as MFI in terminal sera. Percentage of $CD69^+$ (**F**), T_{EM} (**G**), and T_{FH} (**H**) $CD4^+$ T cells. **I**. Percentage of GC $B220^+$ B cells. **J.** GN score distribution: Pg4: proliferative GN score 4; Mc3-4: Mesangial cellular score 3 and 4, Mc1-2: Mesangial cellular score 1 and 2, none = no pathology. N = 10 per group. * $p < 0.05$, ** $p < 0.01$.

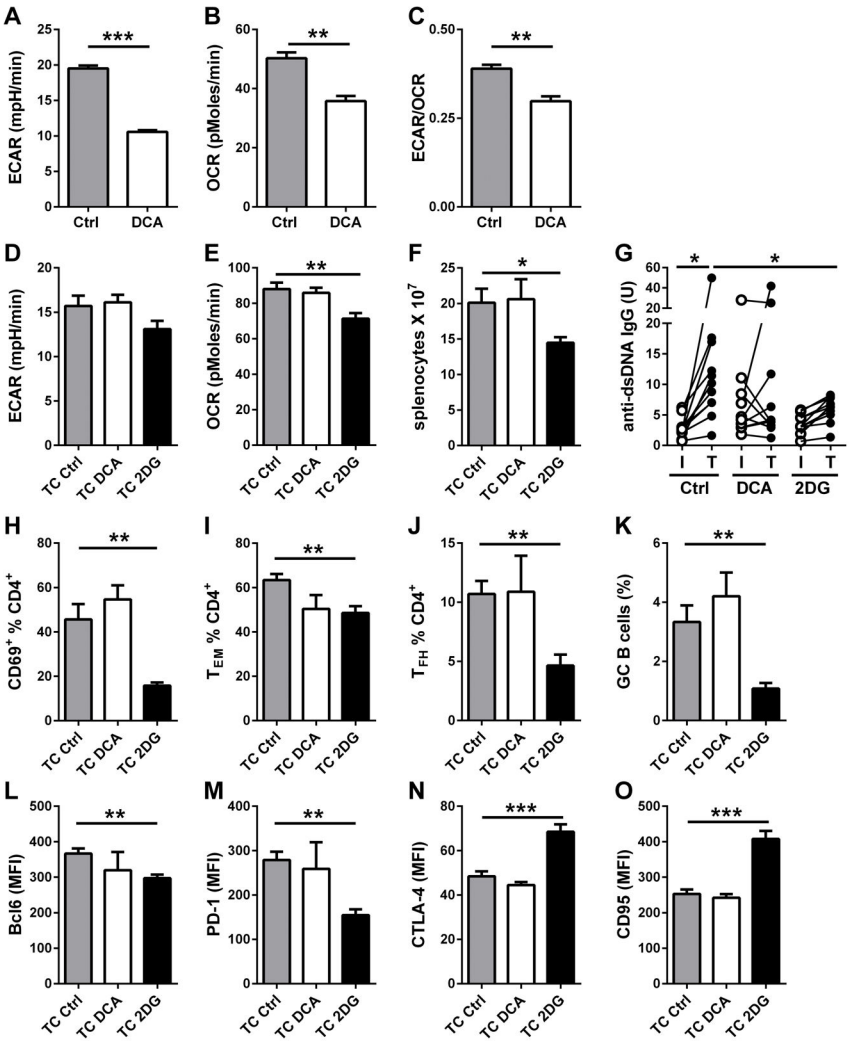

Figure 5. DCA treatment does not reproduce the preventive effect of 2DG. A–C

Effect of DCA (5 mM) on ECAR (**A**), OCR (**B**) and the ECAR/OCR ratio (**C**) of B6 $CD4^+$ T cells after 24 h activation with anti-CD3 and anti-CD28 antibodies (N = 4)**. D–P.** TC mice were treated with DCA or 2DG from 8 to 24 weeks of age, when analysis was performed. $CD4^+$ T cells ECAR (**D**) and OCR (**E**). **F**. Splenocytes numbers. **G.** Serum anti-dsDNA IgG for individual mice with initial (I) and terminal (T) values for each treatment. Percentage of $CD69^+$ (**H**), T_{EM} (**I**), and T_{FH} (**J**) $CD4^+$ T cells. **K**. Percentages GC $B220^+$ B cells. Expression levels of surface makers on total $CD4^+$ T cells: Bcl6 (**L**), PD-1 (**M**), CTLA-4 (**N**) and CD95 (**O**). * $p < 0.05$, ** $p < 0.01$, *** $p < 0.01$. N = 6–10 per group.

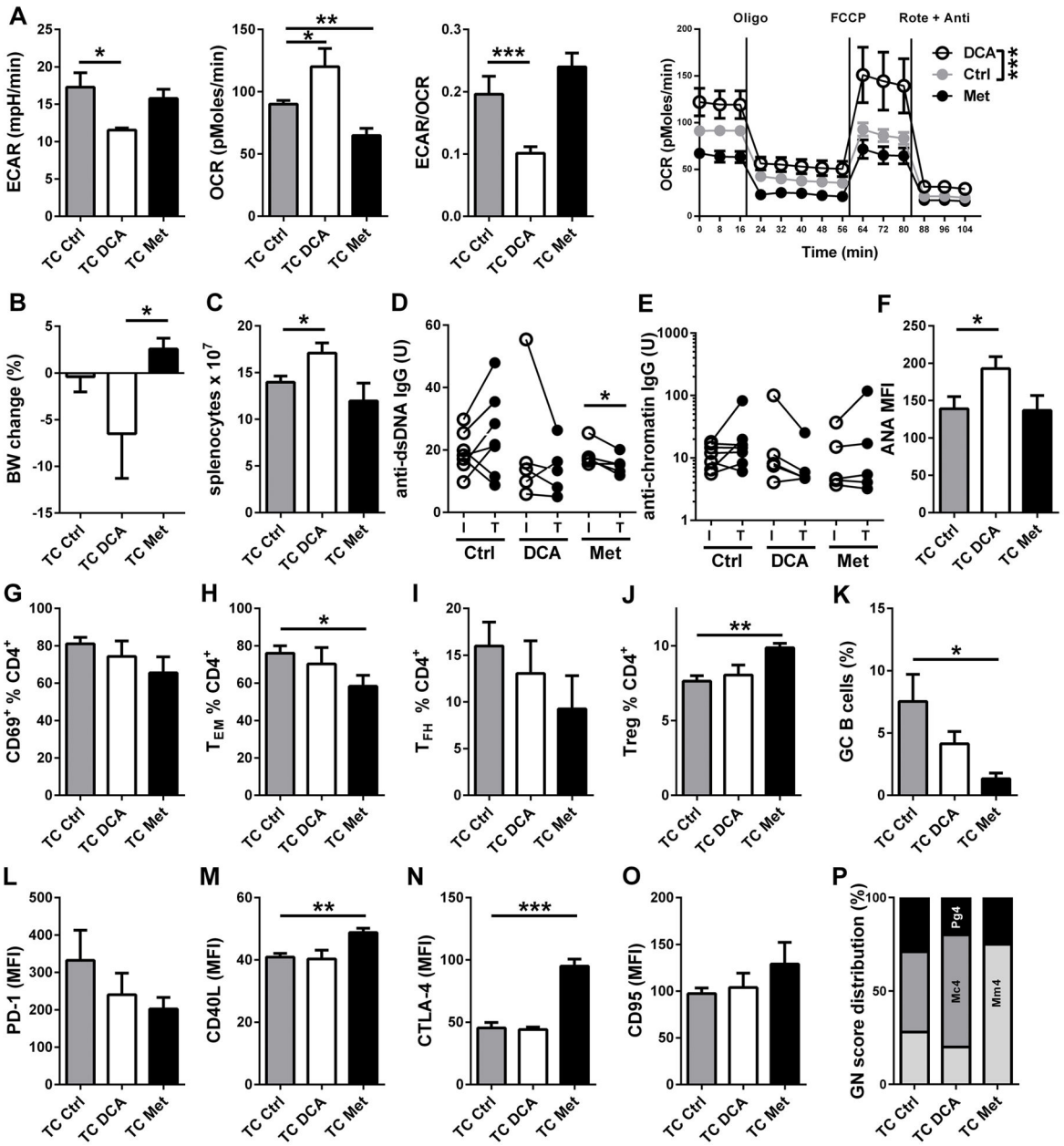

Figure 6. DCA treatment did not reverse disease

8-month old TC mice were treated with DCA or Met for 8 weeks, when analysis was performed. **A**. Effect of treatment on $CD4^+$ T basal ECAR, basal OCR, basal ECAR/OCR ratio, and mitochondrial test OCR plots compared by 2-way ANOVA. **B**. Body weight change during treatment. **C**. Splenocytes numbers. Serum anti-dsDNA (**D**) and anti-chromatin (**E**) IgG for individual mice with initial (I) and terminal (T) values for each treatment. **F**. ANA levels measured as MFI in terminal sera. Percentage of $CD69^+$ (**G**), T_{EM} (**H**), T_{FH} (**I**) and Treg (**J**) $CD4^+$ T cells. **K**. Percentages GC $B220^+$ B cells. Expression levels of surface makers on total $CD4^+$ T cells: PD-1 (**L**), CD40L (**M**), CTLA-4 (**N**) and CD95 (**O**). **P**. GN score distribution: Pg4: proliferative GN score 4; Mc4: Mesangial cellular

score 4, Mm4: Mesangial matrix score 4. N = 10 per group. N = 5–7 per group.* $p < 0.05$, ** $p < 0.01$, *** $p < 0.001$.

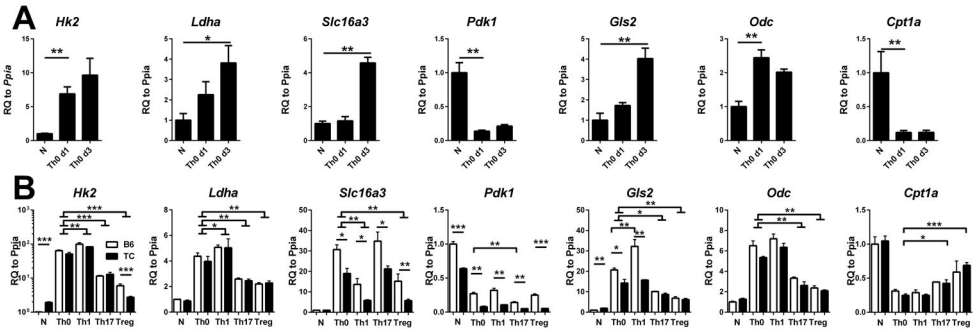

Figure 7. CD4$^+$ T cell activation increased pyruvate oxidation

A. B6 CD4$^+$ T cells were activated with anti-CD3 and anti-CD28 (Th0) for 1 or 3 d, after which metabolic gene expression was compared to unstimulated (N) cells. For clarity, significance values of the 3 d time point were omitted when the difference for d1 was significant. **B**. B6 (white bars) and TC (black bars) CD4$^+$ T cells were activated (Th0) or polarized into Th1, Th17 and Treg conditions for 3 d. Metabolic gene expression was compared to Th0 values. Brackets with horizontal bases indicate significant values for both B6 and TC values. Otherwise, differences were significant for B6 values only (*Pdk1*, *Gls2*) or TC values only (*Cpt1a*). In addition, significant differences between strain for each subset are indicated with horizontal lines. Gene expression in unstimulated (N) cells is shown as reference. Gene expression was normalized to *Ppia*, then to the mean value for N B6 cells. N = 6 per strain. * $p < 0.05$, ** $p < 0.01$. RQ: relative quantity.

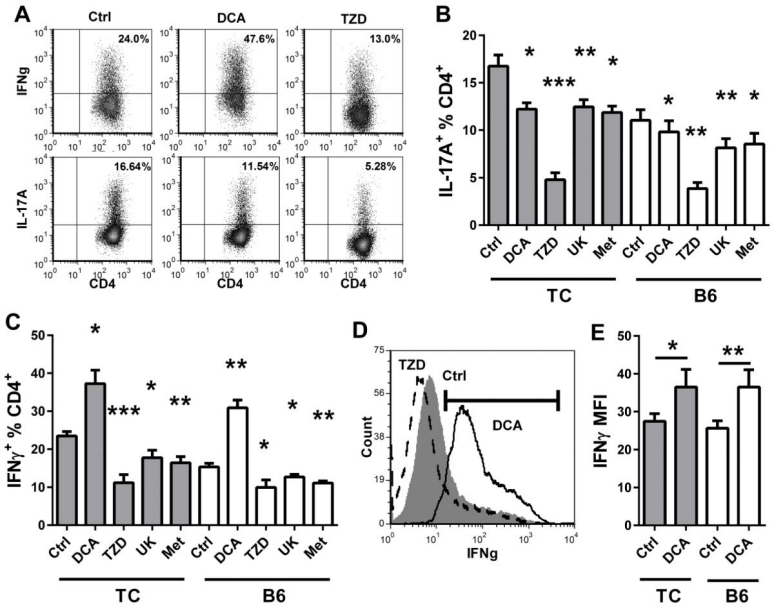

Figure 8. DCA enhanced Th1 polarization

$CD4^+$ T cells from 2 month old TC and B6 mice were polarized in Th1 or Th17 conditions in the presence of DCA, TZD, UK5099 (UK) or Met for 3 d, after which intracellular IL-17A or IFNγ was compared to untreated controls (Ctrl). **A**. Representative IFNγ and IL-17A production in TC $CD4^+$ T cells, Ctrl and treated with DCA or TZD. **B**. Percentage of $IL\text{-}17A^+$ $CD4^+$ T cells. **C**. Percentage of $IFN\gamma^+$ $CD4^+$ T cells. **D**. Representative IFNγ staining in TC $CD4^+$ T cells treated with DCA (solid line), TZD (broken line, and Ctrl (filled histogram). The $IFN\gamma^+$ gate is shown. **E**. MFI of the $IFN\gamma^+$ population as shown in (**D**) for DCA-treated and Ctrl $CD4^+$ T cells. For B and C, comparisons were made to the Ctrl samples in each strain. In E, statistical significance is shown for paired t tests between each treated and Ctrl sample. N = 6 per strain. * $p < 0.05$, ** $p < 0.01$, *** $p < 0.001$.